The caval sphincter in cetaceans and its predicted role in controlling venous flow during a dive

Margo A Lillie[1], A Wayne Vogl[2], Stephen Raverty[3], Martin Haulena[4], William A McLellan[5], Garry B Stenson[6], Robert E Shadwick[1]

[1]Department of Zoology, University of British Columbia, Vancouver, B.C. Canada V6T 1Z4

[2]Department of Cellular and Physiological Sciences, University of British Columbia, Vancouver, B.C. Canada V6T 1Z3.

[3]Animal Health Centre, 1767 Angus Campbell Road, Abbotsford, B.C., Canada V3G 2M3

[4]Vancouver Aquarium Marine Science Centre, PO Box 3232, Vancouver, BC, Canada V6G 3E2

[5]Department of Biology and Marine Biology, University of North Carolina Wilmington, Wilmington, North Carolina, U.S.A

[6]Fisheries and Oceans, Canada, St. John's, NL, Canada A1C 5X1

Corresponding author: lilllie@zoology.ubc.ca

ABSTRACT

A sphincter on the inferior vena cava can protect the heart of a diving mammal from overload when elevated abdominal pressures increase venous return, yet sphincters are reported incompetent or absent in some cetacean species. We previously hypothesized that abdominal pressures are elevated and pulsatile in fluking cetaceans, and that collagen is deposited on the diaphragm according to pressure levels to resist deformation. Here we tested the hypothesis that cetaceans generating high abdominal pressures need a more robust sphincter than those generating low pressures. We examined diaphragm morphology in seven cetacean and five pinniped species. All odontocetes had morphologically similar sphincters despite large differences in collagen content, and mysticetes had muscle that could modulate caval flow. These findings do not support the hypothesis that sphincter structure correlates with abdominal pressures. To understand why a sphincter is needed, we simulated the impact of oscillating abdominal pressures on caval flow. Under low abdominal pressures, simulated flow oscillated with each downstroke. Under elevated pressures, a vascular waterfall formed, greatly smoothing flow. We hypothesize cetaceans maintain high abdominal pressures to moderate venous return and protect the heart while fluking, and use their sphincters only during low-fluking periods when abdominal pressures are low. We suggest pinnipeds, which do not fluke, maintain low abdominal pressures. Simulations also showed retrograde oscillations could be transmitted upstream from the cetacean abdomen and into the extradural veins, with potentially adverse repercussions for the cerebral circulation. We propose that locomotion-generated pressures have influenced multiple aspects of the cetacean vascular system.

INTRODUCTION

The vascular systems of diving mammals are highly adapted to swimming on a breath-hold under high hydrostatic pressures and oxygen deprivation, but there is substantial variation amongst species. One of the more notable adaptations is the presence of a sphincter on the inferior vena cava at the level of the diaphragm. Morphologically, the sphincter in the phocids is the most well developed, formed by a band of striated muscle around the thoracic portion of the vena cava (Fig. 1A) (Harrison and Tomlinson, 1956). Sphincters formed of diaphragmatic muscle that encircles the caval hiatus exist in some otariids (Barnett et al., 1958; Harrison and Tomlinson, 1956) and sea otters (Barnett et al., 1958; Galantsev, 1991). Much less has been reported on caval sphincters in cetaceans. Sphincters have been observed in two relatively fast swimming odontocetes, the harbour porpoise (Barnett et al., 1958; Harrison and Tomlinson, 1956; Hilton and Gaskin, 1978) and bottlenose dolphin (Slijper, 1962), but they are thought either absent or functionally inadequate in the slower swimming fin and sei rorquals (Barnett et al., 1958; Harrison and Tomlinson, 1956; Slijper, 1962). Contraction of the sphincter inhibits caval flow (Elsner et al., 1971; Harrison et al., 1954; Hol et al., 1975), and it has been hypothesized that the sphincter protects the heart from flow overload when venous return is augmented by elevated abdominal pressures (Harrison and Tomlinson, 1956). If this is the case, we wonder why the sphincter should be present in some cetaceans but absent in others.

In cetaceans, the reported variation in sphincter competence parallels variation in the amount of sub-serosal collagen on the cetacean diaphragm (Lillie et al., 2017). This collagen is thought to reinforce the diaphragm to resist deformation under high abdominal pressures while fluking during a dive. We know of no direct measurements of abdominal pressures in a fluking cetacean, but the amount of collagen may provide an index of the abdominal pressures relative to thoracic. (Throughout this paper, the term elevated abdominal pressure will imply a value relative to thoracic pressure.) Cetaceans oscillate their flukes vertically when swimming, compressing the abdomen on each downstroke, and this could generate a series of abdominal pressure pulses throughout fluking (Cotten et al., 2008; Lillie et al., 2017). The amount of

collagen correlates strongly with swim speed expressed as body lengths per second: faster swimming odontocetes like the Dall's porpoise and Pacific white-sided dolphin have ample collagen, but the slower swimming beluga, minke and fin whales do not (Lillie et al., 2017). If this collagen does reflect abdominal pressures, and if the caval sphincter moderates venous flow during periods of elevated abdominal pressures, then animals with high abdominal pressures may need a more robust sphincter than animals with low pressures. This then could account for the reported differences in cetacean sphincter morphology.

The current study examined the need for a caval sphincter in the venous beds of diving mammals experiencing elevated abdominal pressures. We tested the hypothesis that that the need to control venous flow during a dive differs in cetacean species according to the magnitude of their abdominal pressures, and that this is manifest in the morphology of the tissue around the caval hiatus. Since sphincter function has been established in phocids, we studied phocid and otariid diaphragms for comparison. We also developed a model of flow through the inferior vena cava to examine the impact of elevated and pulsatile abdominal pressures on the cetacean venous system and venous return.

METHODS

Details of the animals used in this study are listed in Table 1. Some aspects of their diaphragm morphology have been previously reported (Lillie et al., 2017). Diaphragms were collected at necropsy of animals stranded and recovered along the coast of British Columbia, Canada, by the Marine Mammal Rescue Program or the Marine Mammal Rescue Centre, Vancouver Aquarium, Canada. Specimens were also obtained from the Vancouver Aquarium. Harp seal diaphragms were obtained from Fisheries and Oceans, Canada in Newfoundland. Seals were collected according to the Fisheries Act as part of a biological sampling program. Three fin whale diaphragms were collected from fresh fin whale carcasses as part of a commercial whaling operation at Hvalfjörður, Iceland during the summers of 2013 to 2015. A minke whale diaphragm was obtained from a stranded animal collected by the Marine Mammal Stranding

Program at the University of North Carolina, Wilmington under NOAA stranding permits and was imported to Canada under Convention on International Trade in Endangered Species of Wild Fauna and Flora (CITES) permits. Pig and sheep diaphragms were obtained from local farmers after slaughter for other purposes.

Diaphragms were in excellent to moderate (code 3) post mortem condition and were either examined fresh or frozen at the time of necropsy for later evaluation. Freezing had no apparent effect on the tissue structure. Most of the pericardium, pericardial venous plexus, mesoesophagus and associated connective tissues were removed, but the parietal pleura and peritoneum were generally left intact. The oesophagus and inferior (posterior, caudal) vena cava were frequently absent from the samples. Diaphragms that did not lie flat were draped over a flexible plastic support for study. Tissue morphology was examined using gross dissection. For smaller species, muscle and collagen fibre orientation was verified under a dissecting microscope, as necessary. Two sets of muscles were of interest in this study: the muscles immediately around the inferior vena cava that could act directly as a sphincter, and the muscles at the cranial end of the diaphragm that lie at a short distance from the inferior vena cava but could nonetheless change diaphragm shape and so affect caval diameter.

Muscle thickness was measured with the tissue lying flat on a hard surface. A small-gauge hypodermic needle was inserted vertically through the muscle and was firmly clamped with a hemostat at the point where it entered the muscle surface. Care was taken to ensure the needle fully penetrated the diaphragm and that no dimpling occurred where it pierced the upper surface. The needle was then withdrawn and the length between its tip and the bottom of the hemostats was recorded by photographing the needle beside a ruler. Thickness was measured at a total of 6 locations: on the left and right sides each for the crural, costal and ventral (sternal) muscles.

Mathematical model of abdominal venous flow

Elevation of abdominal pressure reduces the transmural pressures in the abdominal veins, and because these vessels are collapsible, this affects the flow inside. Veins are essentially circular in cross-section under a positive transmural pressure, but start to flatten as transmural pressures fall, increasing resistance to flow. Although the basic hemodynamic relationship $\Delta P=QR$ (where P is pressure, Q is flow, and R resistance) remains applicable under partial collapse (Badeer and Hicks, 1992; Katz et al., 1969), flow cannot be described by the Poiseuille equation, which assumes a circular cross section and does not take into account the reduction of cross-sectional area. Flow can still be modeled mathematically (Holt, 1969; Katz et al., 1969), but this requires more exact knowledge of the collapsing vessel's geometry than is generally available. In an uncollapsed vessel, flow is proportional to the pressure difference between the vein inlet and outlet, but when the vein is partially collapsed, flow becomes proportional to the difference between inlet pressure and external pressure. This change in ΔP between the uncollapsed and partially collapsed states has been used as a basis to model flow (Takata et al., 1990). Flow in the partially collapsed vessel is independent of the outlet pressure, and as a result this phenomenon is widely referred to as a "vascular waterfall". Although the appropriateness of the analogy has been criticized (Badeer and Hicks, 1992), and some prefer the term "Starling resistor", we follow the literature and use waterfall in this paper.

To understand the impact of elevated abdominal pressure on venous flow, we adapted a mathematical model that simulates experimentally observed responses of the dog abdominal venous vasculature (Takata et al., 1990). The model is described fully in that paper. The lumped parameter model consists of an upstream, extra-abdominal bed and a downstream, abdominal bed emptying into the abdominal inferior vena cava (IVC) and then into the thoracic portion of the inferior vena cava (Fig. 1B). The upstream and downstream beds have compliances of *Cu* and *Cd* and experience internal venous pressures *Pu* and *Pd* respectively. Flow between the upstream and abdominal compartments is impeded by the resistance *Ru*, and between the abdominal and thoracic compartments by the resistance *Rd*. Veins in the abdominal

compartment are subjected to a variable tissue pressure *Pab*, and veins in the extra-abdominal compartment are subjected to a constant tissue pressure that we assumed to be close to ambient ocean pressure, *Pamb*. P_{IVC} is the pressure in the IVC at the level of the diaphragm. All pressures are given relative to ambient pressure.

The model simulates the pressures and flows through the two compartments as a function of time based on the input values for flow into the upstream bed, *Q*, and the pressures P_{IVC}, and *Pab*. Flow from the extra-abdominal bed, *Qu*, depends on the pressure drop between the upstream and downstream compartments,

$$Qu = \frac{Pu - Pd}{Ru}. \qquad (1)$$

Similarly, flow from the abdominal bed, *Qd*, depends on the pressure drop between the downstream compartment and the effective backpressure, *Pb*, at the level of the diaphragm,

$$Qd = \frac{Pd - Pb}{Rd}. \qquad (2)$$

Pb depends on the relative magnitudes of *Pab* and P_{IVC}:

$$Pb = P_{IVC} \quad \text{if } Pab < P_{IVC}, \text{ (zone 3, no waterfall)} \qquad (3)$$

$$Pb = Pab \quad \text{if } Pab > P_{IVC}, \text{ (zone 2, waterfall present)} \qquad (4)$$

Zones 3 and 2 refer to the development of a vascular waterfall, following the literature on pulmonary venous beds (West et al., 1964). From conservation of mass we can write

$$\frac{dVu}{dt} = Q - Qu, \qquad (5)$$

$$\frac{dVd}{dt} = Qu - Qd. \qquad (6)$$

Assuming a constant tissue pressure in the upstream compartment, the volume of each bed will change with the venous transmural pressure according to the capacitance of the bed:

$$\frac{dVu}{dt} = Cu\,\frac{dPu}{dt} \qquad (7)$$

$$\frac{dVd}{dt} = Cd\left(\frac{dPd}{dt} - \frac{dPab}{dt}\right) \qquad (8)$$

where the compliances are defined as *Cu* = d*Vu*/d*Pu* and *Cd*=d*Vd*/d(*Pd*-*Pab*). Combining Eqns 5 and 7 and Eqns 6 and 8 gives

$$Qu = Q - Cu\frac{dPu}{dt}, \quad (9)$$

$$Qd = Qu - Cd\left(\frac{dPd}{dt} - \frac{dPab}{dt}\right). \quad (10)$$

Eqns 9 and 10 show that the outflow from each compartment is the difference between the inflow and the volume stored in that bed as capacitance. Substituting Eqn 1 into Eqn 9 and substituting Eqns 1 and 2 into Eqn 10 and rearranging gives the change in venous pressures with time in each compartment:

$$\frac{dPu}{dt} = \frac{1}{Cu}\left(Q - \frac{Pu - Pd}{Ru}\right), \quad (11)$$

$$\frac{dPd}{dt} = \frac{dPab}{dt} + \frac{1}{Cd}\left(\frac{Pu - Pd}{Ru} - \frac{Pd - Pb}{Rd}\right). \quad (12)$$

Eqns 9 to 12 were solved in Matlab. Pressure in the IVC was held at P_{IVC}=0.4 kPa. Initial mean abdominal pressure was *Pab*=0.1 kPa, on which was superimposed a 1 Hz sinusoidal oscillation with a 0.2 kPa (peak-to-peak) amplitude to simulate fluking. Simulations were run for 60 s, followed by a step increase in mean *Pab* to 0.6 kPa for a total of 120 s or to steady state.

In the original Takata model, input values for flow, compliance, and resistance were obtained experimentally and from the literature to represent the venous beds in a 22 kg dog: *Q*=1 ml/kg/s, *Cu*=75 ml/kPa, *Cd*=113 ml/kPa, *Ru*=0.04 kPa/ml/s, and *Rd*=0.008 kPa/ml/s. Comparable parameter values are not available for any cetacean, but they will differ from those of the dog. Parameter values will vary with body mass (dog or cetacean), because each parameter depends on volume. Additionally, cetacean parameter values may differ from the dog's because of specific vascular adaptations to diving. To deal with this unknown, we ran two groups of simulations. In the first, we assumed the cetacean and dog parameters scaled in proportion to body mass, allowing us to extrapolate the cetacean response from the dog's. We assumed flow and compliance increased in proportion to body mass, and resistance decreased in proportion to body mass. From Eqn 1,2, this leaves pressures independent of body size, which generally agrees with observation (Dawson, 2014; Poulsen et al., 2017). We used the values from Takata without adjustment, and the simulated response could be applied to any sized animal by adjusting flows and volumes in proportion to animal size. No adjustment is

necessary for the simulated pressures. In the second group of simulations, we assumed the parameters did not scale with body mass but changed disproportionately and independently. We examined the impact of relative changes in parameter values for *Cu*, *Cd, Ru*, and *Rd*. The impact of fluking frequency was analyzed and is reported in the Appendix.

RESULTS

Overview

The diaphragms of both terrestrial and diving mammals examined in this study consisted of two major groups of muscles, the crural muscles that originated on the vertebral column and coursed cranially to encircle the oesophagus, and the sterno-costal muscles that originated on the sternum and ribs and coursed centrally (Fig. 2). In terrestrial mammals, the two groups of muscles were joined at a large collagenous central tendon. In diving mammals they were joined at a much reduced but still collagenous costo-crural junction. A collagenous aponeurosis was found at the midline ventral to the oesophagus in some diving animals (Lillie et al., 2017). The inferior vena cava pierced the diaphragm generally right of the midline near the junction of these two groups of muscles (Fig. 2B). In terrestrial mammals, it passed through the central tendon, and so its diameter could not be actively controlled by diaphragm muscle. In all the diving mammals, the caval hiatus was surrounded by a mix of collagen and muscle, depending on the species. The muscle morphology around the caval hiatus is illustrated in Fig. 2B and described below.

Phocids

At the cranial aspect of the phocid diaphragm, the sterno-costal muscles ran radially outwards from the inferior vena cava to the sternum and ribs (Fig. 3A). A band of collagen encircled the inferior vena cava, which would protect the caval diameter from distortion due to contraction of these sterno-costal muscles (Fig. 3A,B). The portion of the thoracic inferior vena cava immediately cranial to the diaphragm was encircled by a band of short muscles that formed a sphincter (Fig. 3B). No sterno-costal diaphragm muscle contributed to the sphincter. This has

been well described by Harrison and Tomlinson (1956). Contraction of these muscles would reduce caval diameter.

Otariids and sea otter

On the cranial aspect of the otariid and sea otter diaphragms, the sterno-costal muscles ran radially, but unlike the phocid diaphragm, some of the ventral muscles inserted on a collagenous aponeurosis lying at the midline (Fig. 3C,E,G). The vena cava emerged to the right of the aponeurosis between sterno-costal muscle bundles. In the Steller sea lion, some of sterno-costal muscle passed dorsomedially to the caval hiatus and formed part of a caval sphincter (Fig. 3C,D). However, the bulk of the sphincter was composed of a short, separate muscle band originating and terminating ventromedially to the inferior vena cava (Fig. 3D). In the California sea lion, the inferior vena cava was encircled by several short muscles originating and terminating ventral to the vessel (Fig. 3F). These muscles were separate and were not sterno-costal. In both Steller and California sea lions, the sphincter muscle extended a short distance over the thoracic portion of the inferior vena cava, and contraction of these muscles would directly reduce caval diameter. In the California sea lion, contraction of the sterno-costal muscles would have little impact on caval diameter.

The inferior vena cava in the sea otter emerged from between two bundles of sterno-costal muscles, passing from the right (Fig. 3G). These bundles formed the dorsal and ventral borders of the hiatus, and in some animals the muscle curved to form the medial border as well. In other animals the medial border was collagenous and merged with the collagen of the aponeurosis and collagen on the abdominal side of the diaphragm (Fig. 3G). No distinct structure formed the lateral border. In two of four animals examined, muscle extended a short distance onto the inferior vena cava itself, but we were unable to identify its origins or establish whether it was sterno-costal muscle. The dominant effect of muscle contraction is likely a reduction of the lateral caval diameter.

Odontocetes

The structure of the muscles on the cranial aspect of the diaphragm was similar in the five odontocete species studied. Fig. 4A,C shows the Pacific white-sided dolphin and Dall's porpoise and Fig. 5A shows a killer whale. Where necessary, muscle orientation was confirmed under a dissecting microscope, and for the Pacific white-sided dolphin, short lengths of string placed on the surface are visible as a record. Unlike the radially oriented sterno-costal muscles of the pinnipeds, the muscle ventral to the hiatus in these odontocetes formed a "V", with the point of the V at the sternum near the midline and the arms terminating laterally on either side of the hiatus (Figs 4A,C, 5A). The ventral muscles on the left and right usually overlapped near the sternum, with the right muscle lying cranial to the left. Costal muscle orientation caudal to these ventral muscles was similar to the pinnipeds.

Annular muscle encircling the inferior vena cava was observed in all specimens where it could be examined, including the relatively fast swimming Pacific white-sided dolphin (Fig. 4A,B), Dall's porpoise (Fig. 4C,D), and harbour porpoise, (Fig. 4E,F), and the slower swimming killer whale (Fig. 5A) and beluga (Fig. 5B-D). Most of the muscle lay as a ring on the diaphragm as opposed to extending out onto the thoracic inferior vena cava as it does in the phocids. Only in the harbour porpoise did we document muscle extending onto the inferior vena cava (Fig. 4F); however, the thoracic portion of the inferior vena cava is generally short, and in most specimens it was cut too close to the diaphragm to be satisfactorily examined. On the diaphragm surface, the inner margins of the annular muscle lay at the inferior vena cava, and the outer margins lay roughly one caval diameter out. In some animals, the rings were clearly composed of several individual muscles (Fig 4B), but it was generally difficult to establish where the muscles ended (Fig 5A). Contraction of the annular muscle would reduce the caval diameter.

Mysticetes

The orientation of the muscle at the cranial aspect of the diaphragm in the two mysticetes species examined, three fin whales and one minke, showed somewhat the same basic pattern seen in the odontocetes (Fig. 6). The basic V-shape formed by the ventral muscles in the odontocete was also visible in the fin whales (Fig. 6A,E) and minke (Fig. 6F). In addition, we observed several superficial muscles that overlay the ventral muscles on the thoracic surface. This muscle structure was different in each fin whale examined. Crossing bundles of ventral or sterno-costal muscles are visible to the right of the hiatus in one fin whale (Fig. 6E) and minke (Fig. 6H). A set of five short muscle bundles spiral over the same region in another fin (Fig. 6C), and to the left of the hiatus in the same animal, about six short muscle bundles overlie perpendicularly oriented bundles of sterno-costal muscle. Activation of this complex cranial muscle would likely affect the calibre of the inferior vena cava, and may alter the shape of the diaphragm at its cranial aspect, but the net action of these superficial muscles is not clear.

The muscle around the mysticete inferior vena cava did not appear as a distinct ring like the odontocetes, but nonetheless, muscle that could function as a sphincter passed dorsally and ventrally around the hiatus, similar to the sphincter observed in the Steller sea lion (Fig. 3C). In both the minke and fin whales, a long bundle of sterno-costal muscle passed from the right, crossing dorsomedially to the inferior vena cava, and inserted on a thick collagenous structure (Fig. 6A,B,F). In addition, and sometimes attaching to the same collagen structure, shorter muscles coursed dorsal (Fig. 6G) and ventral to the inferior vena cava (Fig. 6A,B,F,I). We could not confirm whether this was a single muscle. Contraction of these muscles would close the caval hiatus.

Ventral muscle thickness

In cetaceans, the muscle at the ventral part of the diaphragm tended to be thick (Fig 7A-E), and was significantly thicker than the costal muscle (P<0.0005, paired t-test on 14 animals from 6 species). Ventral and costal thicknesses were not significantly different in the pinnipeds (9

animals from 5 species). Ventral muscle thickness relative to costal varied with cetacean species and tended to be greatest in the Dall's porpoise, Pacific white-sided dolphin, and harbour porpoise, species that showed the highest collagen content on their thoracic diaphragm surface (Lillie et al., 2017). The relationship for 9 individuals for which thicknesses and collagen content could be satisfactorily measured is shown in Fig 7F. Collagen content is given as the percent of the thoracic surface area covered by non-pleural collagen and collagen associated with the costo-crural junction (Lillie et al., 2017). If the collagen is deposited to bear elevated abdominal pressures, as proposed, then it follows that some of the muscle that runs in series with the collagen should be correspondingly thickened.

DISCUSSION

The venous systems of both cetaceans and pinnipeds possess several modifications thought beneficial for aquatic life (Barnett et al., 1958; Ponganis, 2015). However, although there appears to be a set of core adaptations common to both groups, other adaptations are specific to each group and details of some of the core adaptations also are species specific (Fig. 1A). The phocid venous system is the most complex, including a caval sphincter, hepatic sinus (a large venous reservoir immediately caudal to the diaphragm), a large intravertebral extradural vein, and large communicating veins that readily shift blood between the abdominal beds and the extradural vein (Harrison and Tomlinson, 1956; Slijper, 1936). Sea lions have a caval sphincter (Barnett et al., 1958; Harrison and Tomlinson, 1956; King, 1977), and an hepatic sinus that develops in size after birth (King, 1977; Murie, 1874), but they lack an enlarged extradural vein (King, 1977). In cetaceans, Harrison and co-workers described a caval "sling" in a harbour porpoise and a transverse band of diaphragmatic muscle just dorsal to the caval hiatus in fetal sei and fin whales, but they questioned whether these structures acted as effective sphincters (Barnett et al., 1958; Harrison and Tomlinson, 1956). Cetaceans lack an hepatic sinus (Barnett et al., 1958; Harrison and Tomlinson, 1956); however, enlarged hepatic venous reservoirs have been observed in these animals (Hilton and Gaskin, 1978; Slijper, 1962). They possess enlarged extradural veins, but the associated communicating veins are reportedly small (Harrison and

Tomlinson, 1956; Slijper, 1962). Finally, cetaceans possess extensive retia mirabilia (vascular plexuses) within the thorax, vertebral canal, and cranial cavity, (Barnett et al., 1958; Lillie et al., 2013; Mcfarland et al., 1979; Walmsley, 1938), whereas these plexuses are generally lacking in pinnipeds.

These differences in vascular architecture will determine how each species is affected by and can respond to changing abdominal pressures during a dive. Elevated abdominal pressure mobilizes blood from abdominal veins and venous reservoirs into the IVC, augmenting venous return to the heart . Therefore, activating a caval sphincter to limit venous outflow not only protects the heart from overload, but also protects abdominal capacitance reservoirs from substantial volume loss (Harrison and Tomlinson, 1956; Murdaugh et al., 1962; Slijper, 1962; Thornton et al., 2001). For any given species, venous adaptations and sphincter structure may be modified according to the relative importance of these two functions as well as to the magnitude of abdominal pressures experienced.

Caval sphincter morphology does not vary with predicted abdominal pressures

Our current study examined cetacean diaphragms for the existence of a caval sphincter and tested the hypothesis that the sphincter structure correlates with abdominal pressures as inferred from diaphragm collagen content (Lillie et al., 2017). We predicted that the species that lacked collagen and so are thought to experience low abdominal pressures while fluking—the beluga, minke and fin whale—would not need a sphincter, while those thought to have higher pressures—the Dall's porpoise and Pacific white-sided dolphins—would have a well-developed sphincter. Contrary to our predictions, we found all cetaceans had sphincters or muscle around the vena cava, not just some species as previously reported. We found no structural difference in the sphincters of odontocetes regardless of whether their diaphragms possessed ample or scant collagen (Fig. 4 vs 5). We also found muscle around the caval hiatus of minke and fin whales that resembled the sphincter muscle of the otariids and appeared capable of modulating flow. These findings do not support the hypothesis that sphincter structure correlates with pressure differentials across the diaphragm as inferred from collagen

content. The structural similarity of all odontocete sphincters suggests a functional similarity that is not linked to the magnitude of the pressures *per se*. In the rest of this discussion, we therefore consider the probable impact that elevated abdominal pressures have on the venous vasculature of diving mammals to better understand the function of the caval sphincter.

Elevated abdominal pressures can alter venous flow by formation of a vascular waterfall

The impact of elevated abdominal pressures on the venous system has been studied in terrestrial mammals. Elevated abdominal pressures can alter venous flow, pressure, and volume in each of the compartments shown in Fig. 1B (Barnes et al., 1985; Guyton and Adkins, 1954). The upstream and abdominal beds each have capacitance (*Cu* and *Cd*, respectively), and the impact this capacitance has on the response to raising abdominal pressure can be readily appreciated through a thought experiment with a compressible, liquid-filled tube (Spaan et al., 1981). Pushing in on the tube will produce no outflow if its ends are stoppered, but instead pressures within the tube will rise. If the ends are not stoppered, then liquid will flow out in both directions without build-up of internal pressures. Pushing in on the tube—elevating abdominal pressures—mobilizes the liquid in the tube, generating transient flow. The stoppers represent the resistances *Ru* and *Rd* in Fig 1B that hinder retrograde and orthograde flow from the abdominal bed. Since these resistances can have intermediate values between fully open and fully closed, repeated application of external pressures should produce some combination of oscillating pressures and flow. The amplitude of these pressure and flow oscillations should vary inversely and will depend on the values of the beds' resistances and compliances.

If abdominal pressure is elevated to the point of exceeding the internal venous pressure, the downstream portion of the IVC can partially collapse and form a vascular waterfall (Downey and Kirk, 1975; Permutt and Riley, 1963). Where no waterfall exists, flow depends on the pressure difference between the inlet and the outlet; the inlet pressure is the venous pressure in the abdominal bed, *Pd*, and the outlet pressure is the pressure in the inferior vena cava, P_{IVC} (Fig. 1B). When a waterfall forms, flow becomes dependant on the pressure difference between the inlet and the surrounding abdominal tissue, *Pab*. The abdominal venous bed can be in one of three vascular zones (West et al., 1964): In zone 3, *Pab* is lower than P_{IVC}; no

waterfall is present, and flow depends on $Pd-P_{IVC}$. In zone 2, *Pab* is higher than P_{IVC}; a waterfall is present, and flow depends on *Pd–Pab*. In zone 1, *Pab* is excessive, and there is minimal or no flow. The response to repeated external pressures will therefore also depend on whether or not a waterfall forms.

Several studies have reported the formation of a vascular waterfall in the abdominal inferior vena cava in dogs (Doppman et al., 1966; Guyton and Adkins, 1954; Lloyd, 1983; Takata et al., 1990), and humans (Aliverti et al., 2009; Wexler et al., 1968). The formation of a waterfall creates a pressure drop across the collapsed segment. Fig 1C shows the pressures from the femoral vein to the right atrium in a dog in which a segment of the veins has collapsed under elevated abdominal pressure (Guyton and Adkins, 1954). Venous pressures upstream of the collapsed segment are high, slightly above the value of the abdominal pressure, but the pressures on the downstream side are low, and in the right atrium they are raised only slightly above normal. Therefore, in the case of elevated but non-oscillating abdominal pressures, the waterfall plays the role of a sphincter and shields the heart from any consequences of sustained high venous pressures. However, the small increases in right atrial pressures visible in Fig 1C were reported to be greater during the initial phases of increasing abdominal pressure (Guyton and Adkins, 1954). Therefore unsteady abdominal pressures could present risks to the heart that are absent under steady pressures.

Waterfall formation can reduce oscillation of caval flow

There has been limited study of the impact of oscillating abdominal pressures on venous flow. In humans, oscillating abdominal pressures produced pulsatile, retrograde venous outflow from the abdomen into the extremities (Aliverti et al., 2009; Aliverti et al., 2010). However, venous pressures were not measured in these studies. The coronary circulation provides an analogous system to study the impact of oscillating external pressures on blood flow, since myocardial contraction increases the tissue pressure around coronary blood vessels. Retrograde flow and the inverse relationship between pressure and flow oscillation amplitude predicted by our thought experiment have been documented experimentally in the coronary beds of dogs

(Spaan et al., 1981) and in an hydraulic model (Westerhof et al., 1983) and a computer model (Lee et al., 1984) of the coronary circulation. In these experiments, conditions were altered by varying the magnitude of an upstream resistor, equivalent to *Ru*. Unfortunately, a waterfall was not consistently maintained throughout the pulse in these studies, allowing the vascular bed to switch between zone 3 and 2 within a beat.

We know of no full analysis of the impact of elevated and oscillating external pressures in zone 2, which we believe could be a relevant state for a fluking cetacean. Since it cannot be directly studied in a cetacean, we adapted a mathematical model developed by Takata et al. (1990). Takata's model simulated the impact of changes in abdominal pressure on venous flow in a dog, and we used it to simulate the impact of oscillating abdominal pressures on flow in a fluking cetacean.

In Fig. 8A-C, we compare the simulated responses in a fluking cetacean first without and then with a vascular waterfall. Parameter values for flow, compliance, and resistance were taken directly from Takata. The simulation starts in zone 3 and shifts into zone 2 with a step increase in *Pab* at t=0. Mean flow at steady-state was kept the same before and after the shift. The panel on the left shows the input pressures for the inferior vena cava (P_{IVC}) and abdomen, plus the simulated pressure responses in the extra-abdominal (*Pu*) and abdominal beds (*Pd*). The middle panel shows the predicted flow through the upstream (*Qu*) and abdominal (*Qd*) beds, and the panel on the right shows the predicted change in venous volume of each compartment (*Vu* and *Vd*) relative to the volume in zone 3. Initially, superimposing oscillations in *Pab* on a low and constant *Pab* (zone 3) yielded oscillations in *Pd* and *Qd* in the abdomen, as anticipated, but also oscillations in *Qu* and, to a small extent in this case, in *Pu* in the upstream compartment (Fig. 8A,B). A step increase in *Pab* that switched the system into zone 2 mobilized some (but not all) of the venous capacitance blood in a single, large flow transient (Fig. 8B). Thereafter, fluking while maintaining an elevated *Pab* (zone 2) produced negligible oscillations in *Qd*, even though the oscillations continued unabated in *Pd*, *Qu* and *Pu*.

The simulated response in Fig. 8B identifies a clear advantage for a fluking cetacean to be in zone 2. When abdominal pressures are low (zone 3), blood is predicted to spurt out of the abdomen into the right heart on each downstroke. When abdominal pressures are sufficiently high to form a waterfall (zone 2), flow out of the IVC is greatly smoothed due to a shift in the phase between oscillations in the two factors that determine *Qd* — inflow into the abdominal bed and the volume stored there as capacitance (Eqn 10). Since there are no flow spurts in zone 2, there is no need for a sphincter to protect the heart against flow overload. Formation of a vascular waterfall not only protects the heart from a sustained, non-oscillating elevated *Pab* (Fig 1C), but it also has the potential to protect the heart from an oscillating *Pab* as well. A caval sphincter, therefore, could be unnecessary for a cetacean while in zone 2. Thus, it is possible that the formation of a vascular waterfall obviates problems arising from oscillating abdominal pressures transmitted to the heart via the IVC. Importantly, however, the simulations also show that, whether or not a waterfall forms, pressure and flow oscillations are transmitted into the upstream vasculature. These oscillations could spread to the thorax via the extradural veins and the superior vena cava.

Diversion of flow into the superior vena cava via paracaval routes is important for maintaining venous return to the heart, particularly when the caval sphincter is contracted (Ponganis et al., 2006), or when abdominal veins are compressed either by elevated abdominal pressures (Doppman, 1967) or external forces (Blix, 2011). In cetaceans, the large diameter of the extradural veins indicates their capacity for a large contribution to venous return, but the simulations show it may also leave them vulnerable to vascular oscillations. If this is the case, the venous system has likely adapted and minimized the impact. The amplitude of oscillations transmitted into the upstream beds was affected by the bed's compliance and resistance: *Ru* had an inverse impact on upstream flow oscillations, and *Cu* had an inverse impact on upstream pressure oscillations (Fig 8E,F). *Ru* encompasses the small communicating veins that link the abdominal bed with the extradural veins, and *Cu* encompasses the very low capacitance of the extradural veins. Keeping *Ru* high minimizes oscillations in flow, but it would also hinder the use of the extradural veins as an alternate route for venous return. Keeping *Cu* high minimizes

oscillations in pressure, but it would also increase flow oscillation (Fig 8E). The model assumes locomotion affects only abdominal pressures, but should locomotion directly compress part of the upstream bed as well, a high *Cu* would particularly exacerbate flow oscillations.

It is not known how cetaceans optimize these parameter values. The flow and pressure oscillations shown in Fig 8E illustrate the conditions that might be encountered in the extra-abdominal beds of a fluking cetacean, including the extradural veins. Switching into zone 2 may simply transfer any potential risks associated with elevated abdominal pressure from the IVC to the superior vena cava, but with the added danger of placing the fluctuations near the brain. Here we suggest the vascular retia mirabilia may provide a solution to this problem. Nagel et al. compellingly demonstrated the pressure-damping effect of the thoracic and spinal retia on the cerebral circulation of bottlenose dolphins (Nagel et al., 1968). However, they did not identify any source of potentially damaging pressures. We hypothesize that potentially adverse pressures generated by fluking are transmitted along the extradural veins and that the retia function as a filter to protect the brain from these pressures.

Use of caval sphincter may differ in cetaceans and pinnipeds

Elevating the abdominal pressure and switching into zone 2 could provide cetaceans with a mechanism to deal with fluking-generated pressure oscillations, but for pinnipeds, being in zone 2 is likely both unnecessary and undesirable. The lateral undulation of phocid swimming and the flipper-dominated locomotion of otariids should not compress the abdomen and generate the same pressure fluctuations as the vertical oscillation of cetaceans (Lillie et al., 2017). In vertical oscillation, the bending axis lies above the thorax and abdomen. Abdominal tissue is alternately compressed and expanded, potentially producing a pressure pulse each downstroke. In lateral oscillation, the axis lies at the midline. One side of the body is compressed while the other expands, with minimal predicted net change in volume or pressure. Additionally, switching into zone 2 yields a volume loss that would make it difficult for a pinniped to maintain blood volume in its hepatic sinus (Fig. 8C). The hypothesis that cetaceans experience high abdominal pressures and associated vascular oscillations and that pinnipeds do not is supported by differences in their morphology. First, diaphragm collagen and muscle

morphology indicate abdominal pressures are higher in cetaceans: extra collagen is present on the cetacean diaphragm but absent on the pinniped diaphragm (Lillie et al., 2017); collagen content correlates with ventral muscle thickness in cetaceans (Fig 7F), and ventral diaphragm muscles in cetaceans are relatively thicker (Fig 7F) and structurally different (Figs 2-5) compared to pinnipeds. Conceivably, the ventral diaphragm muscles could actively generate pressures to shift the abdomen into zone 2. Second, two other morphological features may be interpreted as adaptations to pressure oscillations in the extra-abdominal bed: (1) communicating veins between the abdominal beds and the extradural veins are reportedly small in cetaceans but large in pinnipeds, which would minimize extradural flow oscillations in cetaceans, and (2) the retia are well developed in cetaceans but absent in pinnipeds. These differences in cetacean and pinniped morphologies are consistent with the hypothesis that cetaceans, but not pinnipeds, experience locomotion-generated pressure oscillations in their vascular systems and develop higher abdominal pressures when swimming.

If abdominal pressures do differ between cetaceans and pinnipeds, it is likely there are differences in how they use their caval sphincters. The right heart of any mammal swimming in zone 3 (no waterfall) risks overload from flow transients generated by sudden increases in abdominal pressure (Fig 8A,B). Since both pinnipeds and cetaceans swim while in this zone, both need a caval sphincter. If pinnipeds remain in zone 3, as hypothesized, sphincter use is likely continual. Further, their sphincter controls the volume loss from the hepatic sinus (Elsner et al., 1971; Harrison et al., 1954; Hol et al., 1975; Nordgarden et al., 2000; Ronald et al., 1977; Thornton et al., 2001), and this may explain why the pinniped sphincter is well developed, particularly in phocids. Cetaceans lack the hepatic sinus. In them, the sphincter would be needed to protect the heart when swimming in zone 3 or during the transition from zone 3 to 2. But once in zone 2, the waterfall would protect it from any pressures generated by sustained fluking, making a sphincter unnecessary. This usage in cetaceans could explain, first, why all cetaceans studied possessed a sphincter, and second, why its morphology did not correlate with swimming speed, as we originally anticipated.

General conclusion

All marine mammals must adjust cardiovascular function to meet the needs of exercising during a dive, and they must do this not only with limited oxygen supply but also under changing internal pressures that are potentially adverse to cardiovascular homeostasis. Any hemodynamic adjustment to deal with locomotion-generated pressures must be integrated with other aspects of an animal's dive response, and so the dive response in cetaceans and pinnipeds may differ accordingly. Our simulations show that oscillations in venous return through the cetacean IVC can be moderated by elevating abdominal pressures to create a vascular waterfall. This particular consequence of high abdominal pressures is advantageous, but other consequences need further consideration. How does shifting into zone 2 affect a cetacean's regulation of venous return? How is any redistribution of abdominal venous blood integrated with the redistribution of blood flow as part of the dive response? Where is the mobilized blood stored? In the future, it will be necessary to clearly define how vasculature in the cranial and thoracic compartments can be protected from oscillations generated by locomotion.

APPENDIX

Impact of fluking frequency

Cetaceans fluke at a wide range of frequencies, from as low as 15 strokes min^{-1} in fin whales up to 200 in some dolphins (Fish, 1998; Goldbogen et al., 2006; Williams et al., 2015). The simulations shown in Fig. 8 were based on the single fluking frequency of 60 strokes min^{-1}. The question we address here is how broadly these simulations represent the full range of observed fluking frequencies.

In Fig. A1, we show the oscillation amplitude of the simulated pressure *Pd* (A) and flow *Qd* (B) responses for a wide range of fluking frequencies. At low frequencies, amplitude increases with frequency. The solid vertical lines at 30 strokes min^{-1} mark a point where the curves start to

level out, and the responses are essentially unchanged at all higher frequencies. That is, we consider all responses within the blue area to be the same. The broken vertical lines show the frequency used in the simulations in Fig 8, and since they lie within the blue area, the simulated responses of Fig. 8 represent the response for all fluking frequencies above 30 strokes min^{-1}. The responses at lower fluking frequencies will differ in magnitude from those shown in Fig 8 by the extent indicated. Even at the lowest frequencies, flow (but not pressure) oscillations are predicted to be smoothed on entering zone 2 (B).

Since fluking frequency is generally lower in larger animals, we might anticipate that larger species sometimes operate on the changing (leftward) slopes of these amplitude curves. However, the vascular time constant likely also scales with body size. The rate at which the venous system can respond to a change in abdominal pressure is given by its time constant, calculated as the product of a general venous resistance, *R*, and venous compliance, *C*. For the parameter values used in our model, the time constant is 2 s. The inverse of this time constant is 0.5 Hz or 30 strokes min^{-1}, and this coincides with the solid vertical lines in the two panels. That is, the curves level out when the fluking rate exceeds the inverse time constant, and it is the time constant that determines where the blue area begins. In terrestrial mammals, arterial time constants and heart period (inverse of heart rate) follow the same scaling law with body mass (Westerhof and Elzinga, 1991). If the time constants of the cetacean venous system and fluking period (inverse of fluking frequency) also follow the same scaling law, the solid vertical lines and start of blue area will shift to a lower frequency. Larger animals could still operate on the flat part of the curves, and therefore show the same responses as in Fig 8.

Acknowledgements

The authors thank the staff and volunteers of the Vancouver Aquarium and the Vancouver Aquarium's Marine Mammal Rescue Centre, and the Marine Mammal Section, Fisheries and Oceans, Canada, St. John's Newfoundland. We thank Kristján Loftsson and the staff at Hvalur hf, Iceland, Daníel Halldórsson at the Marine and Freshwater Research Institute, Reykjavík, Iceland, and Paul Cottrell, Marine Mammal Coordinator, Pacific Region Fisheries and Oceans Canada. We also thank Marina Piscitelli-Doshkov, Kelsey Gil, and Alex Werth for their assistance in some of the dissections. We also express our sincere gratitude to John Gosline for his substantial contribution to this project from its inception.

Competing interests

No competing interests declared.

Funding

This work was supported by Discovery Grants from the Natural Sciences and Engineering Research Council [RGPIN 312039-13 and RGPAS 446012-13 to R.E.S. and RGPIN 155397-13 to A.W.V.], and National Oceanic and Atmospheric Administration [NA10NMF4390250 to W.A.M.]

References

Aliverti, A., Bovio, D., Fullin, I., Dellaca, R. L., Lo Mauro, A., Pedotti, A. and Macklem, P. T. (2009). The abdominal circulatory pump. *PLoS ONE [Electronic Resource]* **4**, e5550.

Aliverti, A., Uva, B., Laviola, M., Bovio, D., Lo Mauro, A., Tarperi, C., Colombo, E., Loomas, B., Pedotti, A., Similowski, T. et al. (2010). Concomitant ventilatory and circulatory functions of the diaphragm and abdominal muscles. *J. Appl. Physiol.* **109**, 1432-40.

Badeer, H. S. and Hicks, J. W. (1992). Hemodynamics of vascular 'waterfall': is the analogy justified? *Respir. Physiol.* **87**, 205-17.

Barnes, G. E., Laine, G. A., Giam, P. Y., Smith, E. E. and Granger, H. J. (1985). Cardiovascular responses to elevation of intra-abdominal hydrostatic pressure. *Am. J. Physiol.* **248**, R208-13.

Barnett, C. H., Harrison, R. J. and Tomlinson, J. D. W. (1958). Variations in the Venous Systems of Mammals. *Biol. Rev. Camb. Philos. Soc.* **33**, 442-487.

Blix, A. S. (2011). The venous system of seals, with new ideas on the significance of the extradural intravertebral vein. *J. Exp. Biol.* **214**, 3507-10.

Cotten, P. B., Piscitelli, M. A., McLellan, W. A., Rommel, S. A., Dearolf, J. L. and Pabst, D. A. (2008). The Gross Morphology and Histochemistry of Respiratory Muscles in Bottlenose Dolphins, *Tursiops truncatus*. *J. Morphol.* **269**, 1520-1538.

Dawson, T. H. (2014). Allometric relations and scaling laws for the cardiovascular system of mammals. *Systems* **2**, 168-185.

Doppman, J. (1967). Effect of Valsalva maneuver on the inferior vena cava in man. *Invest. Radiol.* **2**, 332-8.

Doppman, J., Rubinson, R. M., Rockoff, S. D., Vasko, J. S., Shapiro, R. and Morrow, A. G. (1966). Mechanism of obstruction of the infradiaphragmatic portion of the inferior vena cava in the presence of increased intra-abdominal pressure. *Invest. Radiol.* **1**, 37-53.

Downey, J. M. and Kirk, E. S. (1975). Inhibition of coronary blood flow by a vascular waterfall mechanism. *Circ. Res.* **36**, 753-60.

Elsner, R., Hanafee, W. N. and Hammond, D. D. (1971). Angiography of Inferior Vena Cava of Harbor Seal During Simulated Diving. *Am. J. Physiol.* **220**, 1155-&.

Fish, F. E. (1998). Comparative kinematics and hydrodynamics of odontocete cetaceans: morphological and ecological correlates with swimming performance. *J. Exp. Biol.* **201**, 2867-77.

Galantsev, V. P. (1991). Adaptational changes in the venous system of diving mammals. *Canadian journal of zoology* **69**, 414-419.

Goldbogen, J. A., Calambokidis, J., Shadwick, R. E., Oleson, E. M., McDonald, M. A. and Hildebrand, J. A. (2006). Kinematics of foraging dives and lunge-feeding in fin whales. *J. Exp. Biol.* **209**, 1231-1244.

Guyton, A. C. and Adkins, L. H. (1954). Quantitative Aspects of the Collapse Factor in Relation to Venous Return. *Am. J. Physiol.* **177**, 523-527.

Harrison, R. J., Tomlinson, J. D. and Bernstein, L. (1954). The caval sphincter in Phoca vitulina L. *Nature* **173**, 86-7.

Harrison, R. J. and Tomlinson, J. D. W. (1956). Observations on the venous system in certain pinnipedia and cetacea. *Proceedings of the Zoological Society of London* **126**, 205-234.
Hilton, J. W. and Gaskin, D. E. (1978). Comparative volumes and vascular microanatomy of the intrahepatic venous system of the harbour porpoise, Phocoena phocoena (L.). *Canadian Journal of Zoology* **56**, 2292-8.
Hol, R., Blix, A. S. and Myhre, H. O. (1975). Selective redistribution of the blood volume in the diving seal (Pagophilus groenlandicus). *Rapp. P.-V. Reun. Cons. Int. Explor. Mer* **169**, 423–432.
Holt, J. P. (1969). Flow through Collapsible Tubes and through in Situ Veins. *IEEE Trans. Biomed. Eng.* **BM16**, 274-&.
Katz, A. I., Chen, Y. and Moreno, A. H. (1969). Flow through a collapsible tube. Experimental analysis and mathematical model. *Biophys. J.* **9**, 1261-79.
King, J. E. (1977). Comparative Anatomy of Major Blood-Vessels of Sealions Neophoca and Phocarctos - with Comments on Differences between Otariid and Phocid Vascular Systems. *J Zool* **181**, 69-94.
King, J. E. (1983). Seals of the world. New York: British Museum (Natural History) and Cornell University Press.
Lee, J., Chambers, D. E., Akizuki, S. and Downey, J. M. (1984). The role of vascular capacitance in the coronary arteries. *Circ. Res.* **55**, 751-62.
Lillie, M. A., Piscitelli, M. A., Vogl, A. W., Gosline, J. M. and Shadwick, R. E. (2013). Cardiovascular design in fin whales: high-stiffness arteries protect against adverse pressure gradients at depth. *J. Exp. Biol.* **216**, 2548-2563.
Lillie, M. A., Vogl, A. W., Raverty, S., Haulena, M., McLellan, W. A., Stenson, G. B. and Shadwick, R. E. (2017). Controlling thoracic pressures in cetaceans during a breath-hold dive: importance of the diaphragm. *J. Exp. Biol.* **220**, 3464-3477.
Lloyd, T. C. (1983). Effect of Inspiration on Inferior Vena-Caval Blood-Flow in Dogs. *J. Appl. Physiol.* **55**, 1701-1708.
Mcfarland, W. L., Jacobs, M. S. and Morgane, P. J. (1979). Blood Supply to the Brain of the Dolphin, *Tursiops-truncatus*, with Comparative Observations on Special Aspects of the Cerebrovascular Supply of Other Vertebrates. *Neurosci. Biobehav. Rev.* **3**, 1-93.
Murdaugh, H. V., Pyron, W. W., Wood, J. W. and Brennan, J. K. (1962). Function of Inferior Vena Cava Valve of Harbour Seal. *Nature* **194**, 700-&.
Murie, J. (1874). Researches upon the Anatomy of the Pinnipedia.—Part III. Descriptive Anatomy of the Sea-lion (Otaria jubata). *J Zool* **8**, 501-582.
Nagel, E. L., Morgane, P. J., McFarland, W. l. and Galliano, R. E. (1968). Rete Mirabile of Dolphin - Its Pressure-Damping Effect on Cerebral Circulation. *Science* **161**, 898-900.
Nordgarden, U., Folkow, L. P., Walloe, L. and Blix, A. S. (2000). On the direction and velocity of blood flow in the extradural intravertebral vein of harp seals (Phoca groenlandica) during simulated diving. *Acta Physiol. Scand.* **168**, 271-276.
Permutt, S. and Riley, R. L. (1963). Hemodynamics of Collapsible Vessels with Tone: The Vascular Waterfall. *J. Appl. Physiol.* **18**, 924-32.
Ponganis, P. J. (2015). Diving Physiology of Marine Mammals and Seabirds. Cambridge: Cambridge University Press.

Ponganis, P. J., Stockard, T. K., Levenson, D. H., Berg, L. and Baranov, E. A. (2006). Intravascular pressure profiles in elephant seals: Hypotheses on the caval sphincter, extradural vein and venous return to the heart. *Comparative Biochemistry and Physiology a-Molecular & Integrative Physiology* **145**, 123-130.

Poulsen, C. B., Wang, T., Assersen, K., Iversen, N. K. and Damkjær, M. (2017). Does mean arterial blood pressure scale with body mass in mammals? Effects of measurement of blood pressure. *Acta Physiologica* **DOI: 10.1111/apha.13010**.

Rommel, S. A. and Lowenstine, L. J. (2001). Gross and Microscopic Anatomy. In *CRC handbook of marine mammal medicine*, eds. L. A. Dierauf and F. M. D. Gulland), pp. 129-164. Boca Raton: CRC Press.

Ronald, K., McCarter, R. and Selley, L. J. (1977). Venous Circulation in the Harp Seal (*Pagophilus groenlandicus*). In *Functional Anatomy of Marine Mammals Vol 3*, (ed. R. J. Harrison), pp. 235-270. London: Academic Press.

Slijper, E. J. (1936). Die Cetaceen: vergleichend-anatomisch und systematisch. *Capita Zoologica* **6, 7**.

Slijper, E. J. (1962). Whales / Translated by A. J. Pomerans. New York: Basic Books.

Spaan, J. A., Breuls, N. P. and Laird, J. D. (1981). Diastolic-systolic coronary flow differences are caused by intramyocardial pump action in the anesthetized dog. *Circ. Res.* **49**, 584-93.

Takata, M., Wise, R. A. and Robotham, J. L. (1990). Effects of abdominal pressure on venous return: abdominal vascular zone conditions. *J. Appl. Physiol.* **69**, 1961-72.

Thornton, S. J., Speilman, D. M., Pelc, N. J., Block, W. F., Crocker, D. E., Costa, D. P., LeBoeuf, B. J. and Hochachka, P. W. (2001). Effects of forced diving on the spleen and hepatic sinus in northern elephant seal pups. *Proc. Natl. Acad. Sci. USA* **98**, 9413-9418.

Walmsley, R. (1938). Some observations on the vascular system of a female fetal finback. *Contrib. Embryol.* **27**, 107-178.

West, J. B., Dollery, C. T. and Naimark, A. (1964). Distribution of Blood Flow in Isolated Lung; Relation to Vascular and Alveolar Pressures. *J. Appl. Physiol.* **19**, 713-24.

Westerhof, N. and Elzinga, G. (1991). Normalized input impedance and arterial decay time over heart period are independent of animal size. *Am. J. Physiol.* **261**, R126-33.

Westerhof, N., Sipkema, P. and Van Huis, G. A. (1983). Coronary pressure-flow relations and the vascular waterfall. *Cardiovasc. Res.* **17**, 162-9.

Wexler, L., Bergel, D. H., Gabe, I. T., Makin, G. S. and Mills, C. J. (1968). Velocity of Blood Flow in Normal Human Venae Cavae. *Circ. Res.* **23**, 349-&.

Williams, T. M., Fuiman, L. A., Kendall, T., Berry, P., Richter, B., Noren, S. R., Thometz, N., Shattock, M. J., Farrell, E., Stamper, A. M. et al. (2015). Exercise at depth alters bradycardia and incidence of cardiac anomalies in deep-diving marine mammals. *Nat Commun* **6**.

Table 1. List of animals studied

Family	Species and taxonomic authority	Common name	Age class, no. and sex
Phocidae	*Mirounga angustirostris* (Gill)	Northern elephant seal	Juvenile 1M
Phocidae	*Phoca vitulina* Linnaeus	Harbour seal	Adult 1M
Phocidae	*Pagophilus groenlandicus* Erxleben	Harp seal	Adult 1M 2F
Otariidae	*Eumetopias jubatus* Schreber	Steller sea lion	Sub-adult 1 M
Otariidae	*Zalophus californianus* (Lesson)	California sea lion	Adult 1 M
Mustelidae	*Enhydra lutris* (Linnaeus)	Sea otter	Sub-adult 1M Adult 4M
Phocoenidae	*Phocoena phocoena* (Linnaeus)	Harbour porpoise	Sub-adult 1M 1F Adult 3F 1NA
Phocoenidae	*Phocoenoides dalli* (True)	Dall's porpoise	Sub-adult 1M Adult 1M 1NA
Delphinidae	*Lagenorhynchus obliquidens* (Gill)	Pacific white-sided dolphin	Adult 1M 2F
Delphinidae	*Orcinus orca* (Linnaeus)	Killer whale	Calf 1F
Monodontidae	*Delphinapterus leucas* (Pallas)	Beluga	Adult 1F
Balaenopteridae	*Balaenoptera physalus* (Linnaeus)	Fin whale	Adult 2M 1F
Balaenopteridae	*Balaenoptera acutorostrata* Lacépède	Minke whale	Calf 1M
Suidae	*Sus scrofa* Linnaeus	Pig	Sub-adult 2M
Bovidae	*Ovis aries* Linnaeus	Sheep	Sub-adult 3NA

M, male; F, female; NA, sex not available.

Figures

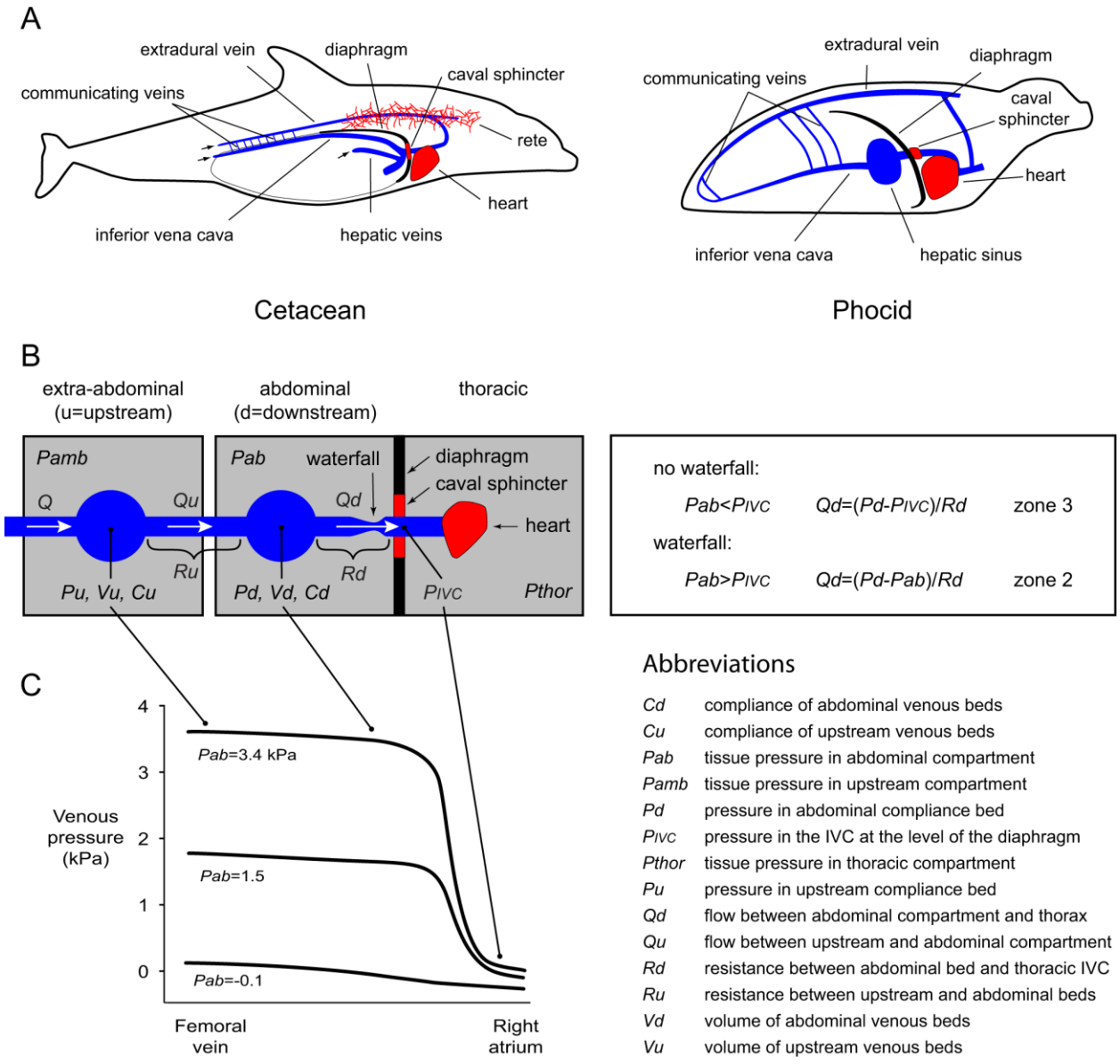

Fig. 1. Schematic diagrams of venous systems. (A) Elements of the cetacean and phocid venous systems. Illustrations are much simplified and not to scale. Adapted from (Rommel and Lowenstine, 2001) with permission, and from (King, 1983) with permission from the Trustees of the Natural History Museum, London. (B) Compartments of abdominal venous system used to

model the impact of abdominal pressures on flow. (C) Venous pressure from the femoral vein to the right atrium of a dog at normal abdominal pressure and at two levels of experimentally elevated abdominal pressure causing venous collapse upstream of the liver. Modified from Guyton and Adkins (1954) with permission.

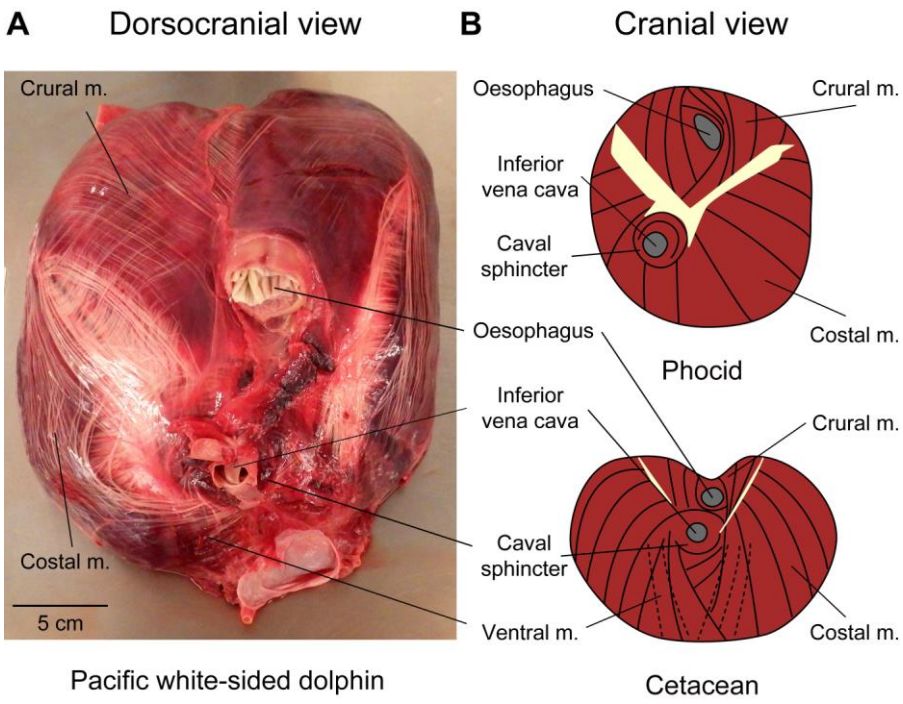

Fig. 2. Morphology of the phocid and cetacean diaphragm. (A) Dorsocranial view of the thoracic surface of Pacific white-sided dolphin showing muscles groups and major structures. The tissue has been draped over a flexible plastic support. (B) Summary diagrams of the thoracic surface of phocid and cetacean diaphragms showing general muscle fibre orientation on thoracic side (solid black lines) and ventral muscle orientation on the abdominal side (broken lines, cetacean only). White indicates collagen at costo-crural junction. Cetacean sub-serosal collagen not shown.

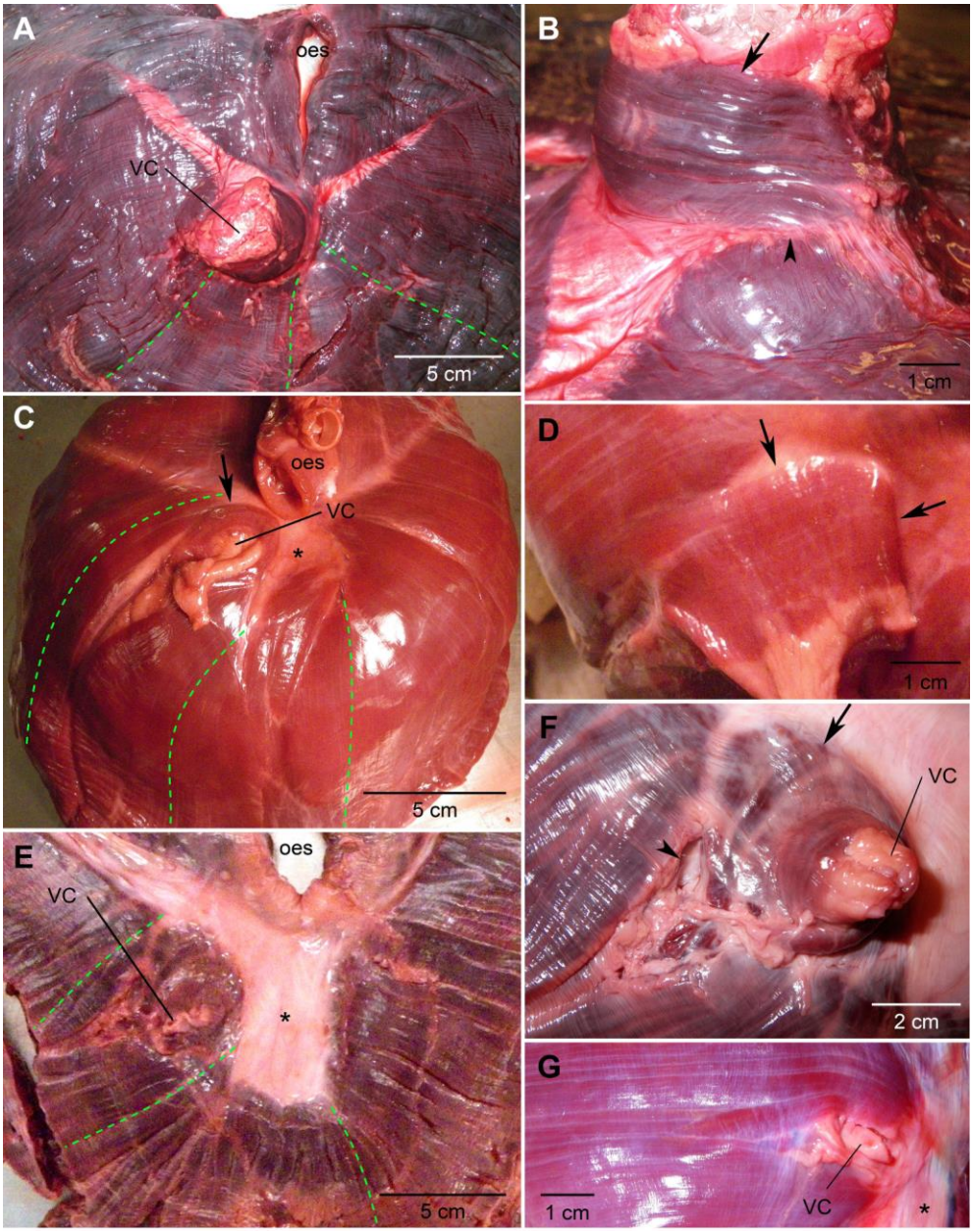

Fig. 3. Thoracic surface of pinniped and sea otter diaphragms showing structure around the inferior vena cava. (A, B) Harp seal. Costal muscle runs radially out from the vena cava (green lines). (B) Side view of caval sphincter showing muscle encircling the vena cava (arrow) separated from the rest of the diaphragm by a ring of collagen (arrowhead). (C, D) Steller sea lion. (C) A slip of costal muscle encircles vena cava (arrow). (D) Dorsal view of caval sphincter. Muscles encircle the vena cava, composed of one band of costal muscle (upper arrow) and a

broader band of muscle originating near the vena cava (lower arrow). (E, F) California sea lion. (E) Costal muscle largely passes above and below the vena cava. (F) Close-up of caval sphincter. A small amount of connective tissue has been removed (arrowhead) to show underlying muscles around vena cava (arrow). (G) Sea otter. Costal muscle passes largely above and below vena cava. VC, vena cava or caval hiatus; oes, oesophagus or oesophageal hiatus; *, collagenous aponeurosis.

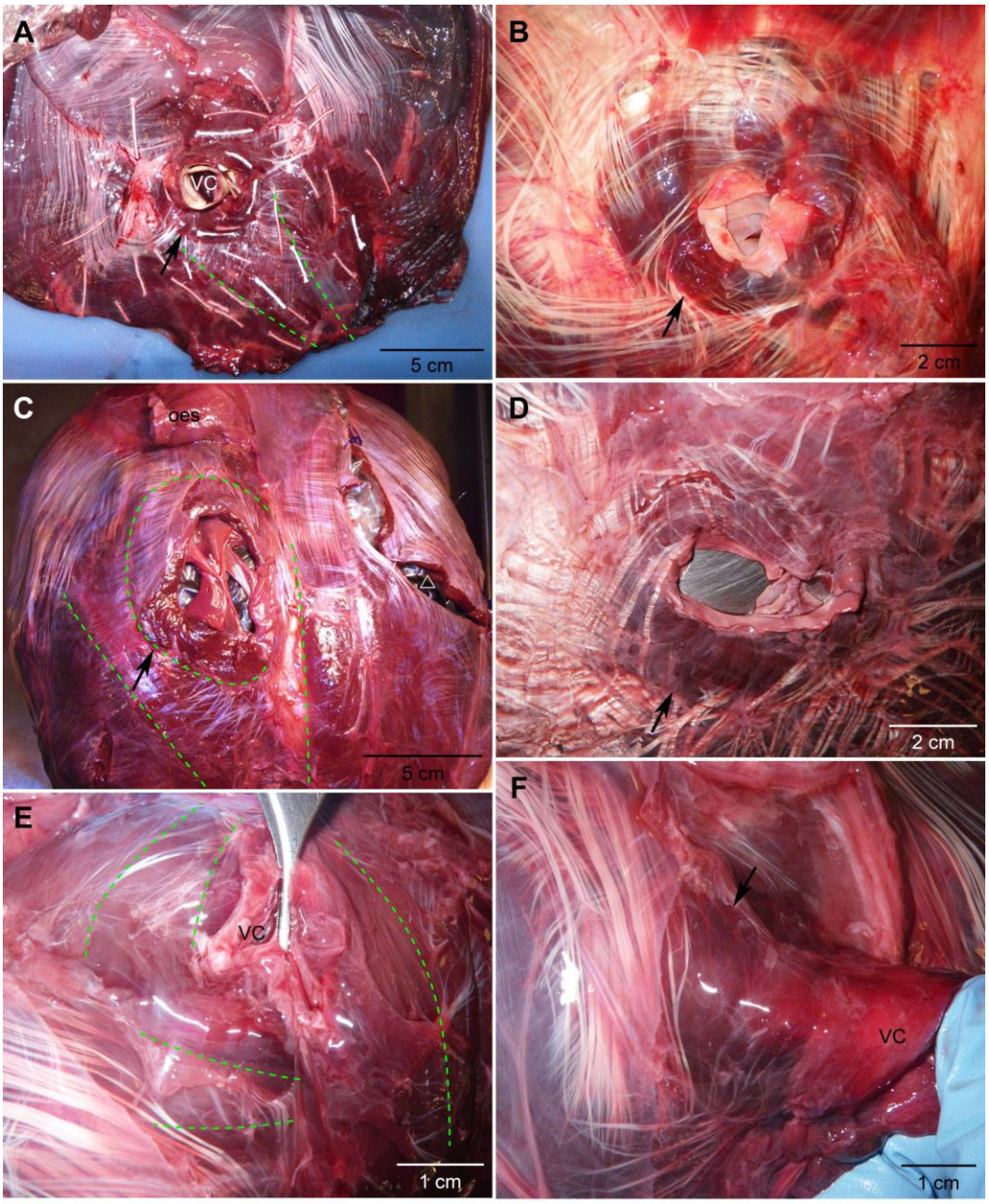

Fig. 4. Thoracic surface of diaphragms showing structure around the inferior vena cava in relatively fast-swimming odontocetes. Two Pacific white-sided dolphins (A, B) and two Dall's porpoises (C, D) showing V-shaped orientation of ventral muscles (green lines) and annular muscle encircling caval hiatus (arrows in A-D and green line in C). Short segments of string have been placed on the surface to show muscle orientation in A. Triangle in C indicates tissue

damaged during necropsy. (E, F) Harbour porpoise. (E) The vena cava is pulled up with forceps to show showing surrounding muscle orientation. (F) Traction on the vena cava shows muscle encircling the vena cava (arrow).

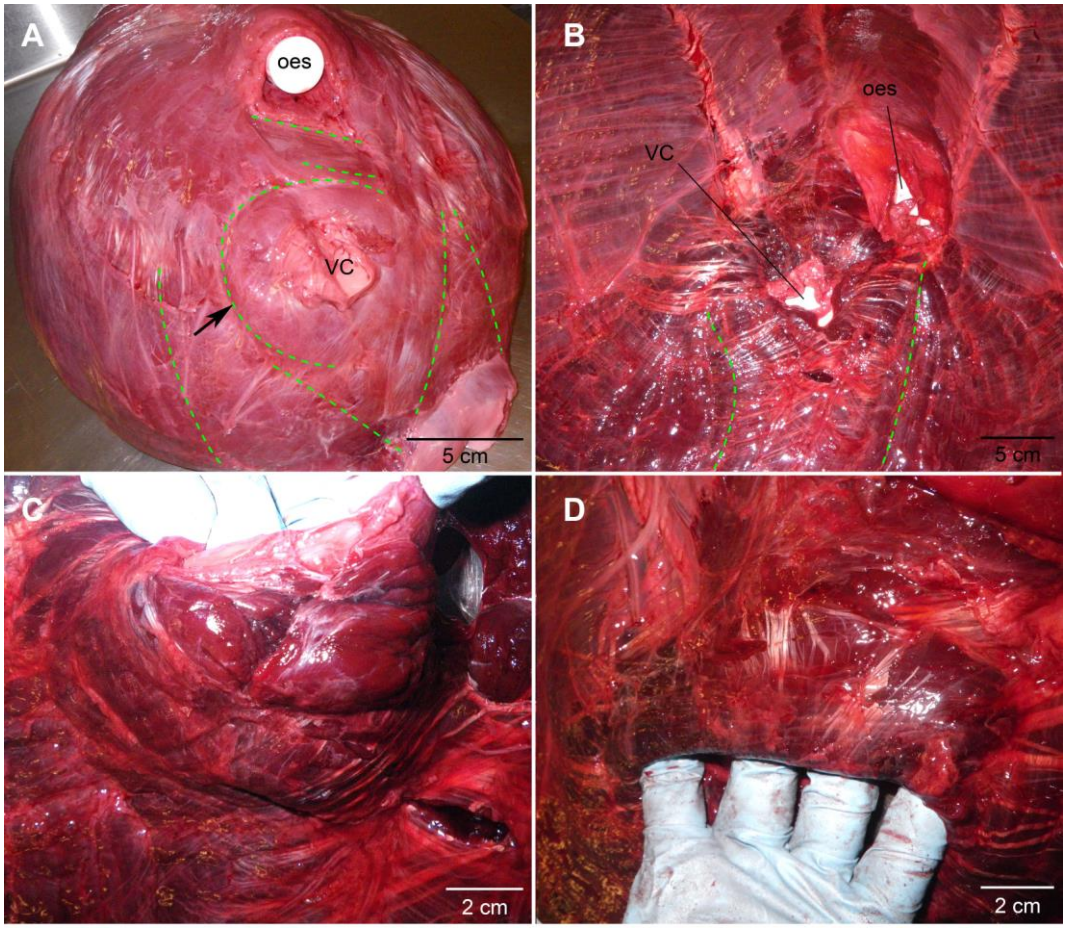

Fig. 5. Thoracic surface of diaphragms showing structure around the inferior vena cava in slower swimming odontocetes. (A) Killer whale showing V-shaped orientation of ventral muscles (green lines) and annular muscle encircling caval hiatus (green line and arrow). (B-D) Beluga. (B) Orientation of ventral muscles is less V-shaped compared to killer whale (green lines). Annular muscle is shown on the ventral (C) and dorsal (D) side of caval hiatus.

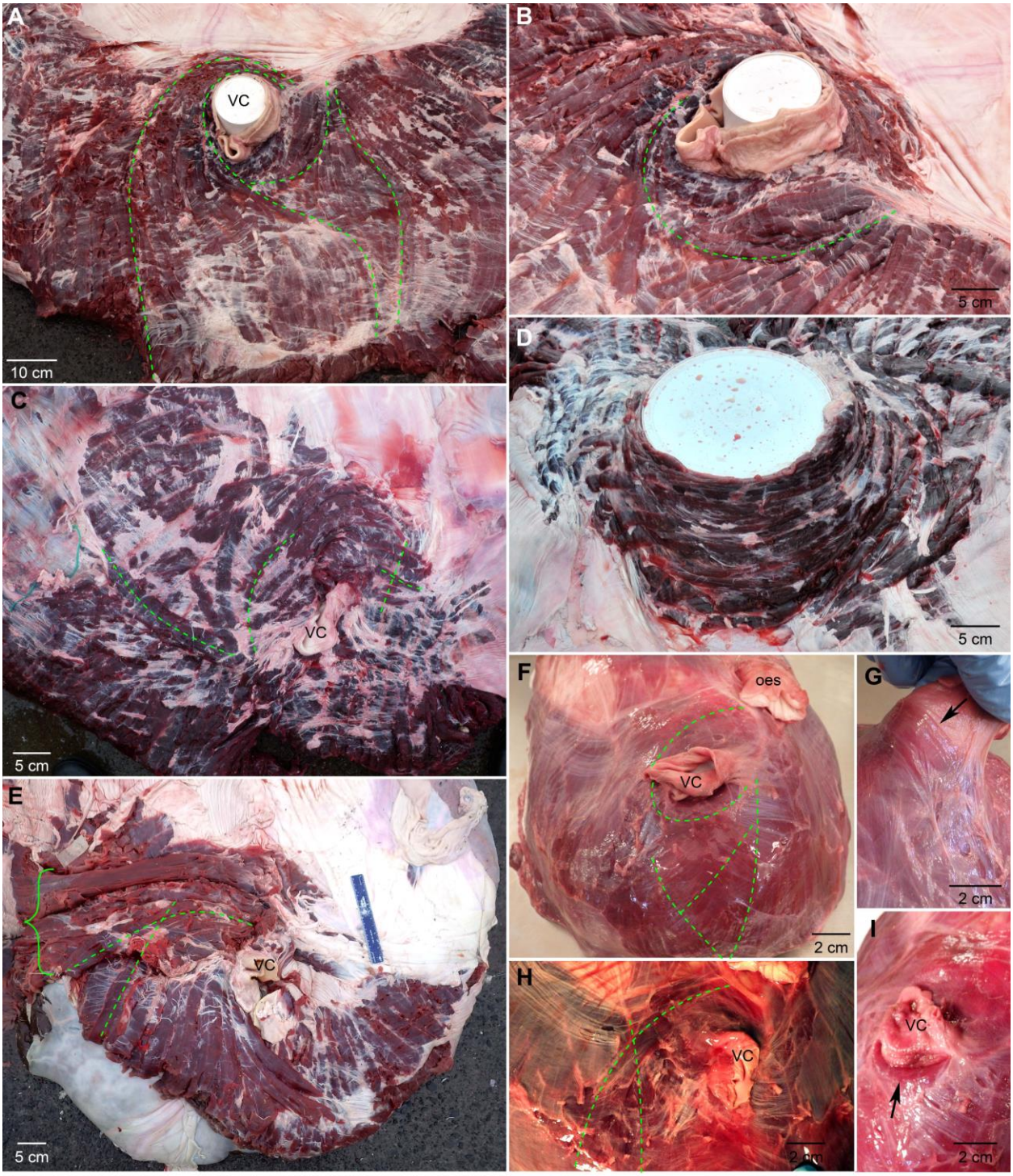

Fig. 6. Thoracic side of diaphragm showing structure around the inferior vena cava in two mysticete species. (A-E) Three fin whales are shown in panels A&B, C&D, and E. A plastic pail has been inserted into the inferior vena cava for clarity in A, B, & D. (A) Muscle orientation is roughly V-shaped with a base near the sternum. (B) Muscle bundles pass dorsal and ventral to the hiatus. (C,D) A spiral of five surface muscles bundles lie to the right of the caval hiatus (two are indicated in green), and an array of short straight muscle bundles run perpendicular to underlying muscles to the left of the hiatus. The muscle dorsal to the hiatus, seen from the dorsal aspect in D, appears continuous with the sternal muscle. (E) Muscular structure around the caval hiatus. The brace indicates a wide band of muscles that runs with a different orientation to underlying muscles. V-shaped orientation of ventral muscles is clear. (F-I) Minke whale. (F) Overview of muscle at the cranial aspect showing V-shaped orientation of ventral muscles. Muscle courses along the dorsal (arrow in G) and ventrolateral (arrow in I) side of vena cava. (H) A band of muscle lateral to the hiatus runs with a different orientation to underlying muscles, similar to the band in E.

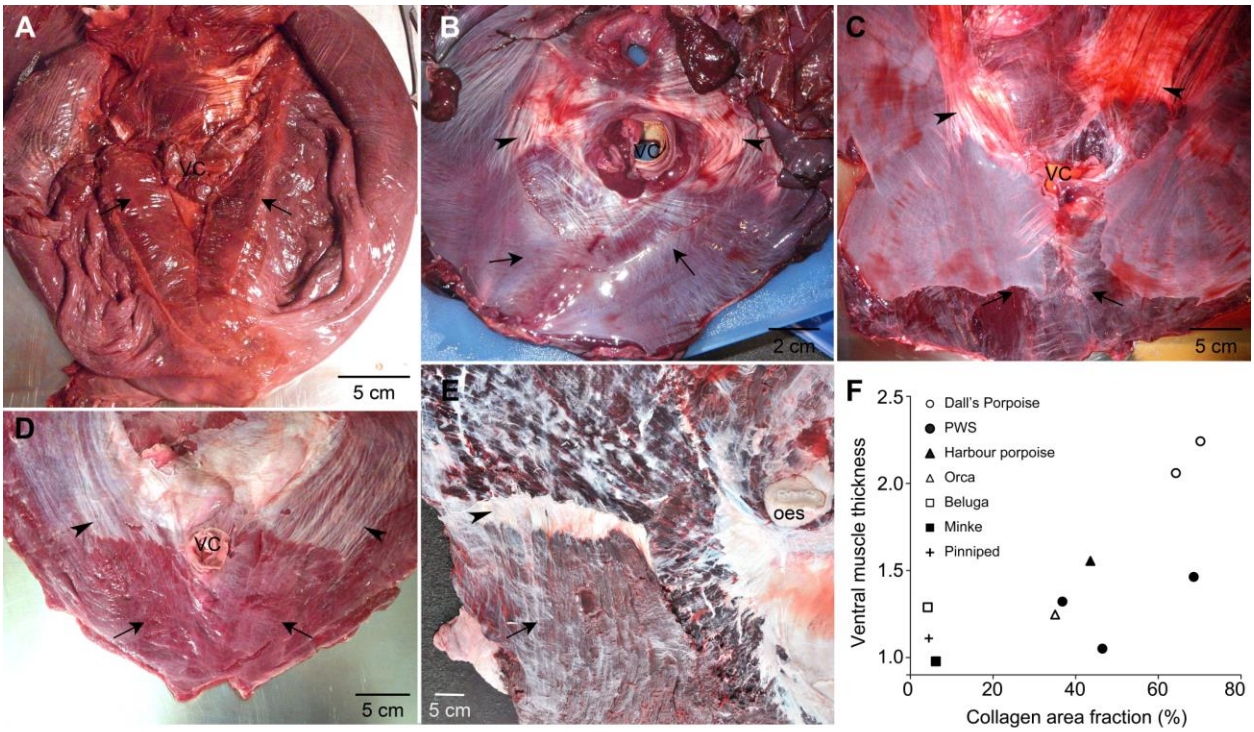

Fig. 7. Abdominal side of diaphragm showing thickness of ventral muscles. Ventral muscles (arrows) are thick in the Dall's porpoise (A) and the Pacific white-sided dolphin (B) relative to the thickness of their costal muscle, and are thinner in the Beluga (C), minke (D) and fin (E) whales. The vena cava for the fin whale lies out of the image to the right. Arrays of collagen fibres run in series with the ventral muscles (arrowheads in B-E). This collagen on the fin whale has been cut. (F) Thickness of ventral muscles relative to costal muscles for that animal correlates with collagen area fraction for that animal. "Pinniped" shows the mean for 9 animals from 5 species, including sea otter.

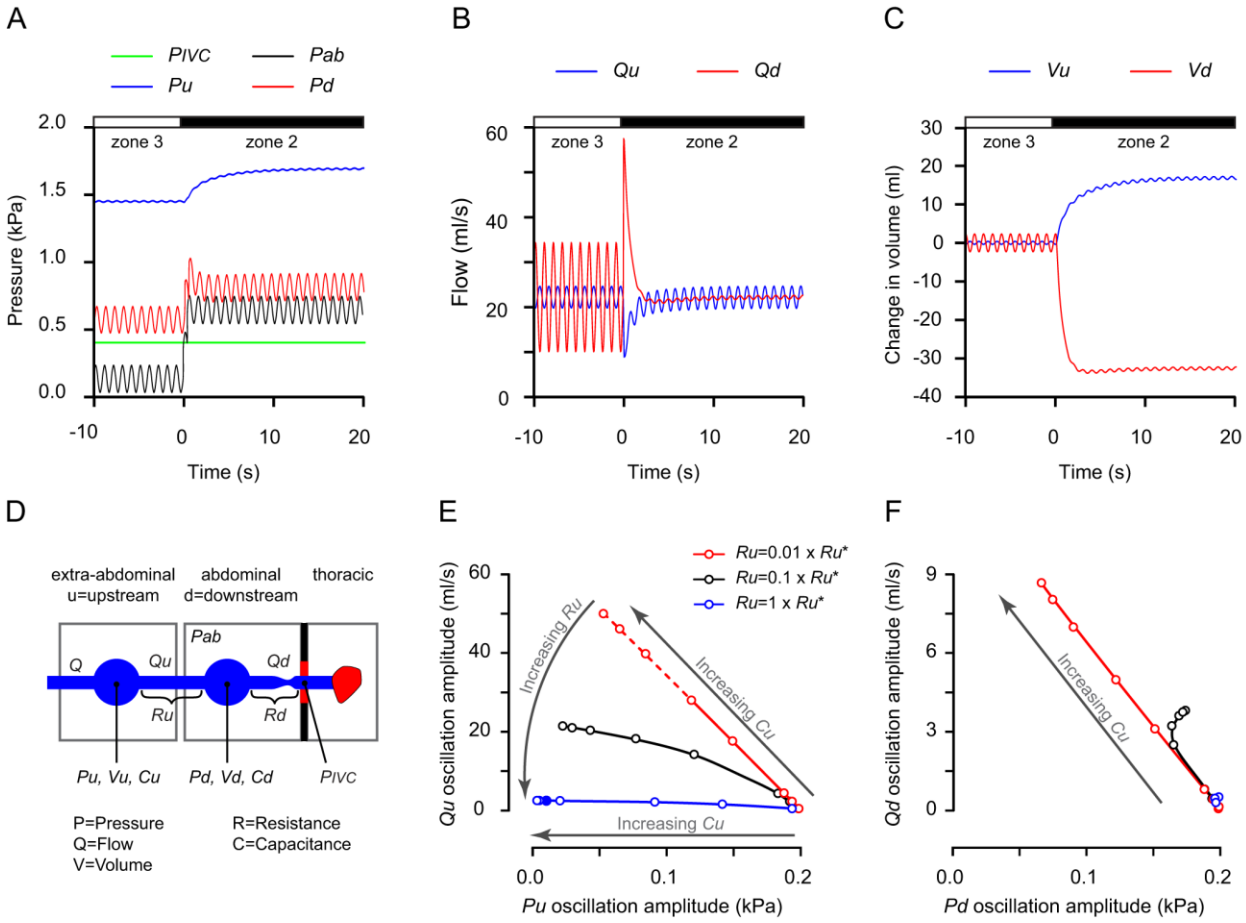

Fig. 8. Simulated response of abdominal venous bed to abdominal pressures in a fluking cetacean. (A-C) Simulation using parameter values from Takata et al. (1990). Abdominal pressures oscillate throughout simulation. At *t*=0 abdominal pressure increases, shifting the vascular bed from zone 3 (no vascular waterfall) into zone 2 (waterfall exists). Oscillations are visible in the abdominal pressure and flow traces and are also transmitted into the upstream, extra-abdominal venous bed. Switching into zone 2 generated a large flow transient in *Qd* and greatly reduced its oscillations, but had little impact on *Pu*, *Pd*, and *Qu*. (C) Formation of a waterfall diminished the volume of the abdominal venous bed and augmented volume in the upstream bed. (D) Schematic summarizing the symbols used. (E-F) Pressure and flow oscillations in the upstream (E) and abdominal (F) beds with different levels of *Cu* and *Ru*

relative to the values reported by Takata, *Ru** and *Cu**. Note the difference in ordinate values. Simulations are shown for three levels of *Ru*, each tested at eight levels of *Cu*, from 0.01 x *Cu** to 4 x *Cu**. The filled circle in D corresponds to the values used in A-C, *i.e.*, *Ru** and *Cu**. Pressure and flow oscillation amplitudes varied inversely. *Ru* had an inverse impact on *Qu* oscillations (ordinate). *Cu* had an inverse impact on *Pu* oscillations (abscissa). For the lowest values of upstream compliance tested, and regardless of the value set for *Ru*, the pressure oscillations in the upstream bed reached the full 0.2 kPa amplitude generated by *Pab* in the simulation.

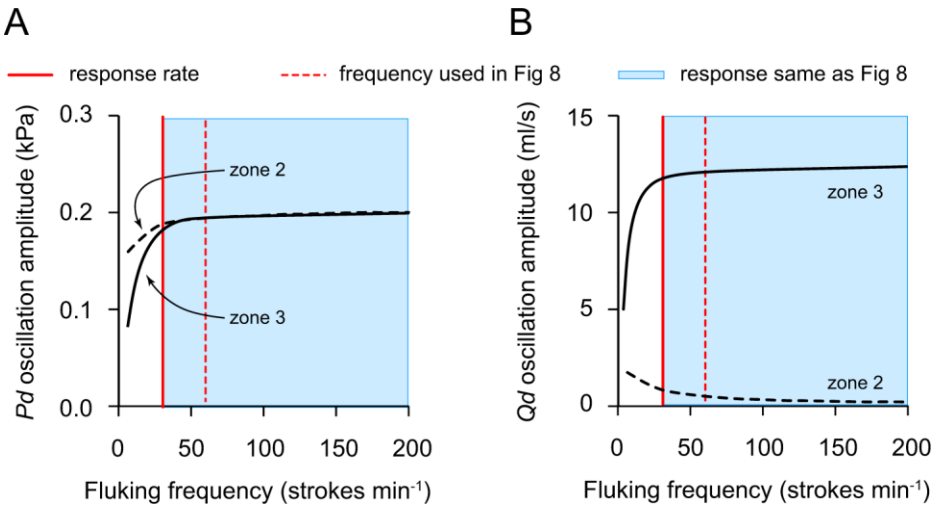

Fig. A1. Simulated effect of fluking frequency on pressure and flow oscillations in abdominal bed. Oscillation amplitudes are insensitive to fluking frequencies above the venous response rate of 30 strokes min^{-1} (solid red line), corresponding to the time constant of 2 s. Simulated responses will be similar for all fluking frequencies above 30 strokes min^{-1} (blue area), including the 60 strokes min^{-1} (broken red line) used in the simulation shown in Fig. 8. Increasing the time constant shifts the response rate line and curve shoulder left, and broadens the frequency range covered by the simulation. Decreasing the time constant has the opposite effect.